JOURNAL OF SOLID STATE CHEMISTRY 107, 117–126 (1993)

The Cuprate $Bi_6Ba_4Cu_2O_{15}$: A Double Collapsed 2201-Type Structure

M. HERVIEU, C. MICHEL, M. T. CALDES,* A. Q. PHAM, AND B. RAVEAU

*Laboratoire CRISMAT, CNRS URA 1318, ISMRA/Université de Caen, Boulevard du Marechal Juin, 14050 Caen Cedex, France; and *Institut de Ciència de Materials de Barcelone, Campus U.A.B., 08193 Bellaterra, Spain*

Received November 13, 1992; in revised form March 3, 1993; accepted March 4, 1993

A new cuprate, $Bi_6Ba_4Cu_2O_{15}$, with a monoclinic symmetry (a = 12.191 Å, b = 5.555 Å, c = 27.00 Å; β = 93.31°) has been isolated. The high-resolution electron microscopy study of this phase has allowed a structural model to be established. The structure is deduced from that of the 2201-modulated superconductor by a double "collapsing operation," and is called for this reason "double collapsed 2201-type" structure. Indeed, a first translation along $\mathbf{c}_{2201}$ of $a_p(1 + \sqrt{2}/2)$, every five octahedral block leads to the hypothetical n = 5-member of the collapsed family (a_p is the parameter of the ideal cubic cell of the perovskite); a second translation performed in the latter structure along $\mathbf{b}_{2201}$ of $a_p\sqrt{2}$ leads to the present structure. In fact, this structure consists of "2201"-type slices, parallel to $(012)_{2201}$, whereas the n = 5 collapsed structure would consist of identical slices but parallel to $(010)_{2201}$. The analogy of these crystallographic collapsed structures with the crystallographic shear structures suggests the existence of two families of structures characterized by two kinds of crystallographic collapsing planes (CCP), $\{010\}_{2201}$ and $\{012\}_{2201}$, respectively. The oxides $Bi_{17}Sr_{16}Cu_7O_{49-\delta}$ and $Bi_{15}(Sr, Ba)_{14}Cu_6O_{42}$ represent the members n = 8 and 7 of the first family called collapsed, whereas the cuprate $Bi_6Ba_4Cu_2O_{15}$ represents the member n = 5 of the second family called 2201-type double collapsed.

Introduction

The recent investigations of the Bi–Sr–Cu–O system have shown its very complicated chemistry due to the existence of the redox couples, Bi(III)/Bi(V) and Cu(II)/Cu(III), and to the stereoactivity of the $6s^2$ lone pair of Bi(III). As a result, the ideal structure of the superconductor $Bi_2Sr_2CuO_6$ called 2201 (*1*), built up from the intergrowth of a triple rock salt layer with a single perovskite layer (Fig. 1a), has never been stabilized. The actual structure exhibits an incommensurate modulation (Fig. 1b), resulting from a modulated displacement of the atoms coupled with a modulated substitution of bismuth for stontium, leading to a monoclinic supercell (*2–8*). Another consequence is the existence of three other structural families in the Bi–Sr–Cu–O system, which are stabilized by a small variation of the cations contents with regard to the ideal cationic ratio 2 : 2 : 1 of the 2201 ideal structure. The structures of the different families can be easily described from the 2201 structure. The first family corresponds to the "orthorhombic tubular" oxides. The structure of these phases results from the intergrowth, along the $\mathbf{b}_{2201}$ axis of the 2201 structure, of $n[Bi_2Sr_2CuO_6]_\infty^{2201}$ with a perovskite-related layer $[Sr_8Cu_6O_{16}]_\infty$ (Fig. 1c). In that way, there exist two types of perovskite layers in the structure: in the first one, the 2201 unit is parallel to (001) and, in the second, the $[Sr_8Cu_6O_{16}]_\infty$ unit is parallel to (010). At the connection of the two perovskite layers, square tubular tunnels are formed, running along [100] and partly filled up with disordered oxygens (*9, 10*). Four members of the orthorhombic tubular family were isolated

0022-4596/93 $5.00

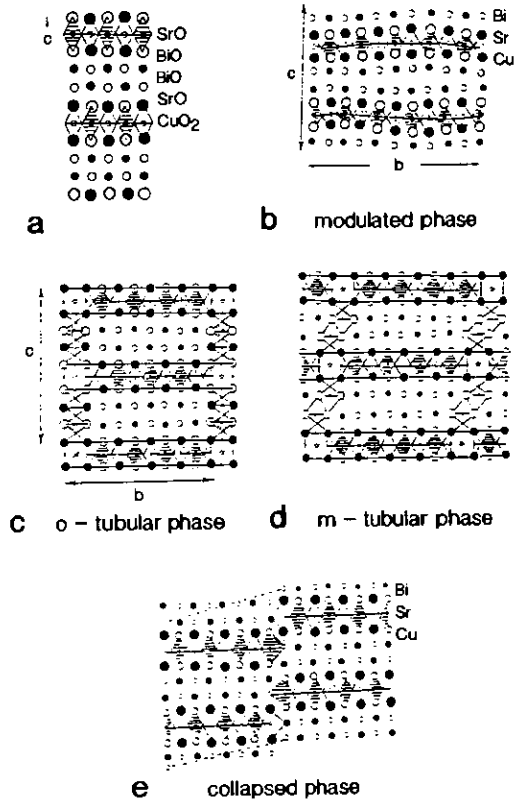

FIG. 1. Schematic drawing of the structure of bismuth-based cuprates related to "2201": ideal 2201 (a); modulated "2201" (b); orthorhombic tubular phase, $n = 7$ (c); monoclinic tubular phase, $n = 7$ (d); and collapsed phase, $n = 8$ (e).

(*11*), corresponding to the general formulation $(Bi_{2+x}Sr_{2-x}CuO_6)_n(Sr_8Cu_6O_{16+y})$ with $n = 4, 5, 6, 7$.

For a composition close to $n = 7$, with a slight excess of bismuth, a second phase (*12*) was observed representative of the second family. The structure of this oxide is closely related to the orthorhombic tubular $n = 7$ oxide. It can be described from the latter by a translation of one layer $[BiO]_\infty$ with regard to the adjacent one, leading to a monoclinic cell (Fig. 1d). As soon as the n value is high, ($n \geq 6$), numerous intergrowth defects are observed (*13*) resulting from the stacking along **b** of different n members.

The third family was discovered for a composition corresponding to $Bi_{17}Sr_{16}Cu_7O_{49-\delta}$ (*14, 15*). A structural model, based on high resolution electron microscopy observation (*14*) was proposed, showing close relationships with the 2201-type structure. The structure of this phase (Fig. 1e) is deduced from that of 2201 by a translation along **c** of eight 2201-type blocks along **b**, i.e., $[Bi_2Sr_2CuO_6]_8$, leading to a monoclinic cell; such a phase was designated by the authors "collapsed" phase by comparison with the 2201-ideal structure.

Contrary to the Bi–Sr–Cu–O system, the Bi–Ba–Cu–O system has only been recently investigated. This comes from the fact that reactions performed in oxidizing atmosphere lead most of the time to the partial oxidation of Bi(III) into Bi(V), stabilizing the perovskite $BaBiO_3$ (*16*). For this reason barium-based bismuth systems were recently investigated using an inert atmosphere (*17–19*). With this method of synthe-

sis, a mixed barium strontium bismuth cuprate $Bi_{15}(Sr, Ba)_{14}Cu_6O_{42}$ was isolated (*20*). This oxide belongs to the third family, i.e., its structure is deduced from that of 2201 by a similar translation along **c** to that observed for $Bi_{17}Sr_{16}Cu_7O_{49-\delta}$ but of seven 2201-blocks instead of eight; thus, both oxides $Bi_{15}(Sr, Ba)_{14}Cu_6O_{42,5}$ and $Bi_{17}Sr_{16}Cu_7O_{49-\delta}$ belong to the "collapsed" family with general formula $(Bi_2A_2CuO_6)_n(Bi_{4+x}A_4Cu_{2-x}O_{12+x/2})$ and represent the members $n = 7$ and 8, respectively (*20*).

The recent synthesis of 2201-type barium-based cuprates (*17–19*) suggested that the Ba–Bi–Cu–O system is a potential field for the generation of such structural types. The present paper reports on the synthesis of a new cuprate, $Ba_4Bi_6Cu_2O_{15}$, with an original structure, closely related to the 2201-structure, and that will be called "double collapsed" phase.

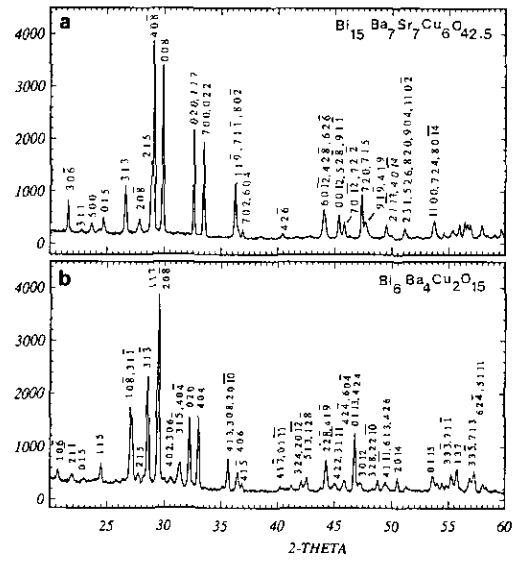

FIG. 2. XRD patterns of (a) $Bi_{15}Ba_7Sr_7Cu_6O_{42.5}$, the collapsed phase $n = 7$, and (b) $Bi_6Ba_4Cu_2O_{15}$, the double collapsed phase.

Experimental

The samples were prepared starting from Bi_2O_3, $Ba(NO_3)_2$, and CuO. The mixtures were crushed in an agate mortar and pressed in the form of pellets. They were heated at 800°C, under a nitrogen flow, for 24 to 48 hr.

The X-ray diffraction patterns were registered using a Seifert vertical diffractometer equipped with a primary monochromator in order to select Cu $K_{\alpha 1}$ radiation. Data were collected by step scanning with increment of 0.02° (2θ) in the range 15–80°C (2θ). Lattice constants were determined and structural calculations were performed using the profile refinement computer program DBW3.2 (*21*).

The electron diffraction study was performed with a JEOL 200 CX electron microscope, fitted with an eucentric goniometer (+60°). The high resolution study was performed with a TOPCON 002 B electron microscope, operating at 200 kV. The aberration constant of the objective lens is 0.4 mm. The samples were prepared by a smooth crushing of the oxides in *n*-butanol; the theoretical images were calculated using the EMS program (*22*). The EDAX analysis was performed with a KEVEX analyzer mounted on the TOPCON electron microscope.

Results

For the composition $Bi_6Ba_4Cu_2O_{15}$, a new phase is isolated. The powder X-ray pattern (Fig. 2b) exhibits strong similarities with that of $Bi_{15}(Ba, Sr)_{14}Cu_6O_{42,5}$ (Fig. 2a). The electron diffraction study confirms that a single phase is obtained. The reconstruction of the reciprocal space evidences a monoclinic cell with $a \sim 12$ Å, $b \sim 5.5$ Å, $c \sim 27$ Å, and $\beta \sim 93°$; the characteristic [010] electron diffraction pattern is shown in Fig. 3. The conditions limiting the reflections lead to the A_2, A_m, $A_{2/m}$ possible space groups. Note that weak streaks along A and weak extra spots on the electron diffraction patterns are observed in some crystals.

The cell parameters were refined from the XRD data to the following values:

$a = 12.191\,(1)$ Å, $b = 5.555\,(1)$ Å,

$c = 27.001\,(3)$ Å, and $\beta = 93.31°\,(1)$.

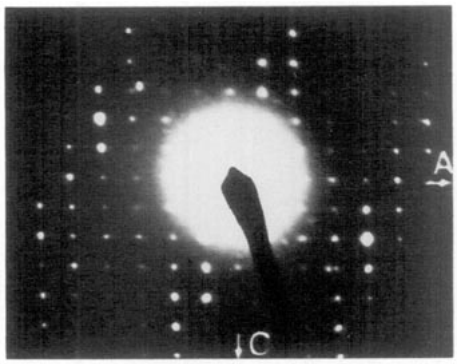

FIG. 3. [010] electron diffraction pattern of $Bi_6Ba_4Cu_2O_{15}$.

Owing to the similarity of the XRD patterns with the $n = 7$ member of the "collapsed" family, the structure was expected to be that with a lower n value. However, if we calculate the theoretical parameters (*20*) of such members, $n \leq 5$, it appears clearly that they do not fit with the experimental ones and, thus, this hypothesis could be rejected.

In order to understand the atomic arrangement which occurs in this oxide, we have performed a high-resolution study. The crystals exhibit a mica-like morphology with a [011] prefered orientation. Referring to the bismuth layered cuprates, the [010] orientation was chosen for study.

A typical [010] image (Fig. 4) shows that the contrast consists in undulating rows of white dots with a very regular periodicity. This shows that the streaks and weak spots in the E.D. patterns are not due to extended defects.

In a first step, the contrast was interpreted with the help of the observed and calculated images obtained for the 2201 modulated phase (*23*) and the tubular and the collapsed phases (*11, 13, 15, 20, 24*). The striking feature of this contrast deals with the oval-shaped arrangement formed by two adjacent segments of brightest spots (Fig. 4): the two segments are further separated at the center and get closer to each other at their ends. The examination of a region around each oval shaped double segments (delimited by a square on Fig. 4) shows that on both sides of these segments, a second row of bright dots is observed, which undulated in accordance with the oval-shaped rows. The first rows of brightest dots forming oval shaped segments are attributed to $[BiO]_\infty$ layers and the second rows to the $[BaO]_\infty$ layers. The dark rows which separate these units are attributed to the copper layers which are often not highlighted in the bismuth-layered cuprates. Thus it is observed that locally each small region around the oval-shaped segments corresponds to a staking of layers, according to the sequence "BaO–BiO–BiO–BaO–CuO_2," i.e., characteristic of the 2201 structure. Along the direction of the rows (see black arrow, Fig. 4), one observes that the double oval-shaped segments consist of five bright spots and form staggered rows along that direction, two adjacent oval-shaped segments being shifted with respect to each other in the perpendicular direction. As a result each $(BiO)_5$-type segment is connected at one end by a $(BaO)_n$ segment and at the other end by a $(CuO_2)_n$ segment. The contrast of one undulating rows of spots along the b_{2201} direction is characterized by the sequence of five brightest dots, nine less bright spots, five bright dots, five darker spots which can be attributed to the sequence "$(Bi)_5$–$(Ba)_9$–$(Bi)_5$–$(Cu)_5$." In fact the contrast of the dots at both ends of the copper segments is brighter than for the three other spots of the segment, suggesting that these terminal sites are partly occupied by bismuth. In the same way the barium sites may be partly occupied by bismuth. This contrast is similar to that observed in the collapsed phase and suggests that the shifting mechanisms is kept. The contrasts of the two types of phases differ when looking in the direct perpendicular to the layers. In the "collapsed" phases, the double oval-shaped segments formed by the bismuth atoms stay in a straight line along the direction perpendicu-

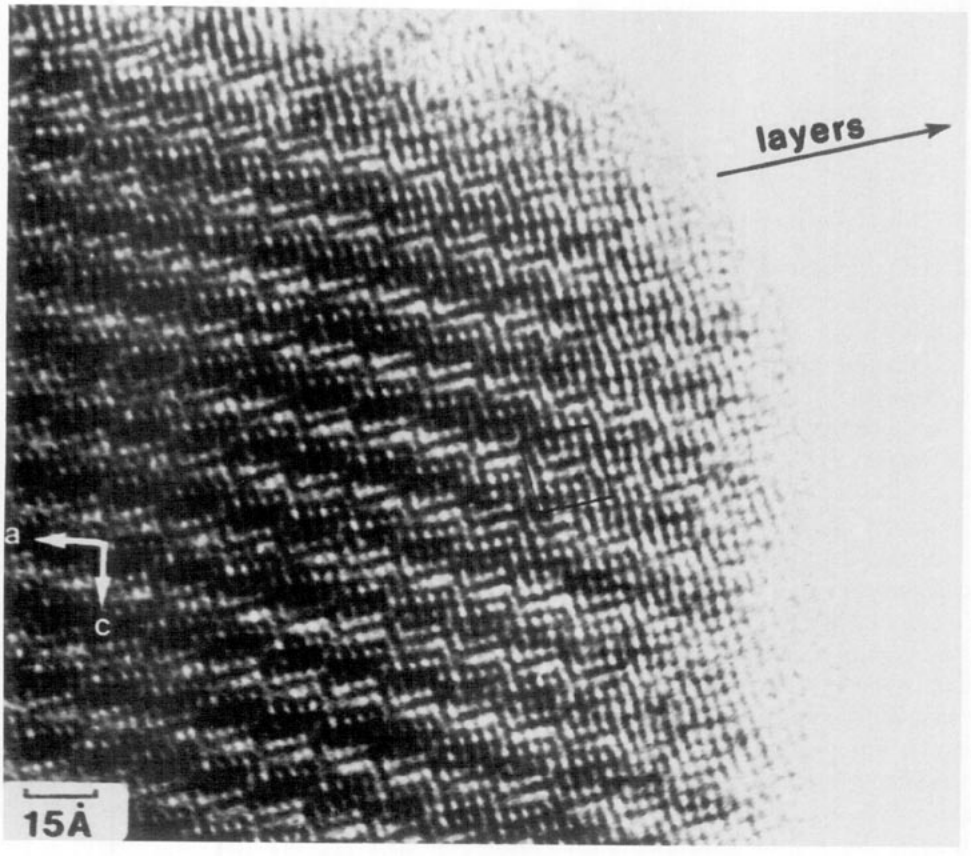

FIG. 4. Typical [010] HREM image of $Bi_6Ba_4Cu_2O_{15}$. The oval-shaped double segments are delimited by a square.

lar to the layers; in $Bi_6Ba_4Cu_2O_{15}$, each oval-shaped segment is translated of $a_p\sqrt{2}$ in a direction parallel to the layers.

From these observations a structural model can be proposed (Fig. 5) which corresponds to an "ideal" stacking of identical undulating layers along c_{2201}. Such layers parallel to the $(001)_{2201}$ plane, would be built from three kinds of ribbons according to the sequence $[(BiO)_5(BaO)_9BiO)_5(CuO_2)_5]$. Such a theoretical model would lead to the composition $Bi_{10}Ba_9Cu_5O_{29}$. In fact, the EDAX analysis performed in about thirty crystals leads to a cationic content close to the nominal composition, i.e., $Bi_{12}Ba_8Cu_4O_{30}$. This result is quite compatible with the variation of contrast observed at the

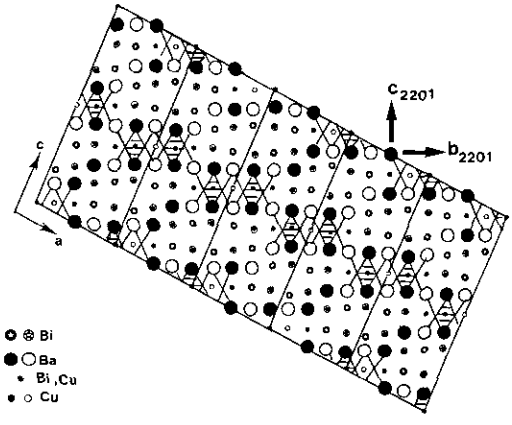

FIG. 5. Ideal model proposed for the structure of $Bi_6Ba_4Cu_2O_{15}$.

ends of the copper segments which suggests that a part of terminal copper sites are occupied by bismuth. Moreover a part of the barium sites may be occupied by bismuth. Thus, each undulating layer would be derived from the ideal one by the sequence

$$[(BiO)_5(Ba_{8/9}Bi_{1/9}O)_9(BiO)_5(Cu_{4/5}Bi_{1/5}O_2)_5].$$

Moreover, a possible exchange between bismuth and barium, especially at the junction of the $(BiO)_5$ and $(Ba_{8/9}Bi_{1/9}O)_9$ should also be considered.

To check the validity of this model it is necessary to compare calculated and experimental images. However the dramatic influence of the cationic positions on the contrast requires one to work with a model as close as possible to the actual structure. Since it appears quite unrealistic to refine such a model which includes 45 heavy atoms and 58 oxygens per cell from powder X-ray data, only the positions of the cations and their distribution were refined in the most symmetric space group $A_{2/m}$.

The refined values of the positional parameters were used for the calculations of the images, the oxygen atoms were then located in ideal positions deduced from the positions of the heavy atoms in order to respect the theoretical interatomic distances. The values used for the image calculations are given in Table I; the projection of the structure, for 2 × 2 cells, is given in Fig. 6. The theoretical images were calculated for different thicknesses of the crystals; an example of through focus series is given in Fig. 7 for t = 33 Å. The calculated images fit remarkably well within the experimental ones. Two examples are given in Figs. 8a and b. In the first one (Fig. 8a), the bismuth and barium atoms are correlated with the dark dots and the double oval-shaped segment is formed by two black segments. In Fig. 8b, the barium and bismuth atoms are highlighted and the oval is then formed from bright dots. It should be noted that in the thicker part of the crystal, the contrast is not drastically changed; the dark zone correlated with the copper layers is only more apparent, in agreement with the calculated images.

TABLE I

$Bi_6Ba_4Cu_2O_{15}$: Atomic Positions Used for the Image Calculations

Element	Site	x/a	y/b	z/c
Bi(1)	4*i*	0.345	0.000	0.877
Bi(2)	4*i*	0.107	0.000	0.339
Bi(3)	4*i*	0.927	0.000	0.801
Bi(4)	4*i*	0.754	0.000	0.259
Bi(5)	4*i*	0.439	0.000	0.570
O(1)	4*i*	0.345	0.500	0.877
O(2)	4*i*	0.107	0.500	0.339
O(3)	4*i*	0.927	0.500	0.801
O(4)	4*i*	0.754	0.500	0.259
O(5)	4*i*	0.439	0.500	0.570
O(6)	2*d*	0.500	0.500	0.000
O(7)	4*i*	0.264	0.500	0.473
O(8)	4*i*	0.033	0.500	0.941
O(9)	4*i*	0.861	0.500	0.404
O(10)	4*i*	0.379	0.500	0.140
O(11)	4*i*	0.435	0.500	0.300
O(12)	8*j*	0.680	0.250	0.448
O(13)	8*j*	0.899	0.250	0.483
Cu(1)	4*i*	0.439	0.000	0.570
Cu(2)	2*b*	0.000	0.500	0.000
Cu(3)	4*i*	0.798	0.500	0.466
Ba(1)	2*c*	0.500	0.000	0.000
Ba(2)	4*i*	0.264	0.000	0.473
Ba(3)	4*i*	0.033	0.000	0.941
Ba(4)	4*i*	0.861	0.000	0.404
Ba(5)	4*i*	0.379	0.000	0.140
Ba(6)	4*i*	0.435	0.000	0.300

Note. Space group: $A_{2/m}$. Cell parameters: a = 12.19 Å, b = 5.556 Å, c = 27.00 Å; β = 93.31°.

Discussion

The comparison of the experimental images with the theoretical images calculated on the basis of the model proposed in Fig. 6 and the atomic positions of Table I attests to the validity of this model. Of course, it will be necessary to refine the positional parameters of the oxygen atoms and the occupancy factors to reach the fine structure from neutron diffraction data.

The structure of the cuprate $Bi_6Ba_4Cu_2O_{15}$ is closely related to those of the 2201-type

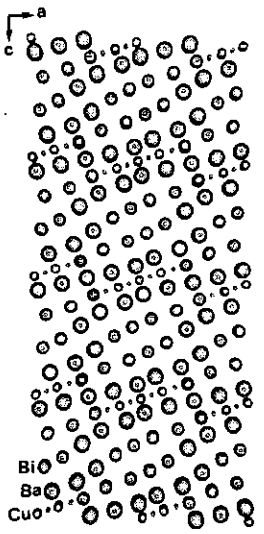

FIG. 6. Projection along [010] of the structure of $Bi_6Ba_4Cu_2O_{15}$ calculated from the refinement of the positional parameters of the cations (Table I). The oxygen atoms are in ideal positions.

phase, $Bi_2Sr_2CuO_6$, and to the $n = 5$ member of the collapsed family $(Bi_2A_2CuO_6)_n$ $(Bi_{4+x}A_4Cu_{2-x}O_{12+x/2})$ which has not been synthesized up to now. The relationships between the three structures are shown in Fig. 9. By shearing the structure of the 2201-cuprate (Fig. 9a) along the **c** direction every fifth CuO_6 octahedron along **b** (see arrows), i.e., by applying a translation $t_c = a_p(1 + \sqrt{2}/2)$ along c_{2201} every fifth octahedron one obtains the $n = 5$-member of the collapsed family (Fig. 9b), the structure is in fact characterized by 2201-type slices which are five octahedra thick. As a result that collapsed phase becomes monoclinic, with an "a" parameter slightly different from that of the orthorhombic cell of the ideal 2201-structure, whereas c and b remain unchanged ($a_{col} \sim \mathbf{a}_{2201}$, $b = \mathbf{b}_{2201}$, $c = \mathbf{c}_{2201}$; $\beta \neq 90°$). Starting from the $n = 5$-member of the collapsed family (Fig. 9c), if one applies a second translation $t_b = a_p\sqrt{2}$ between two lay-

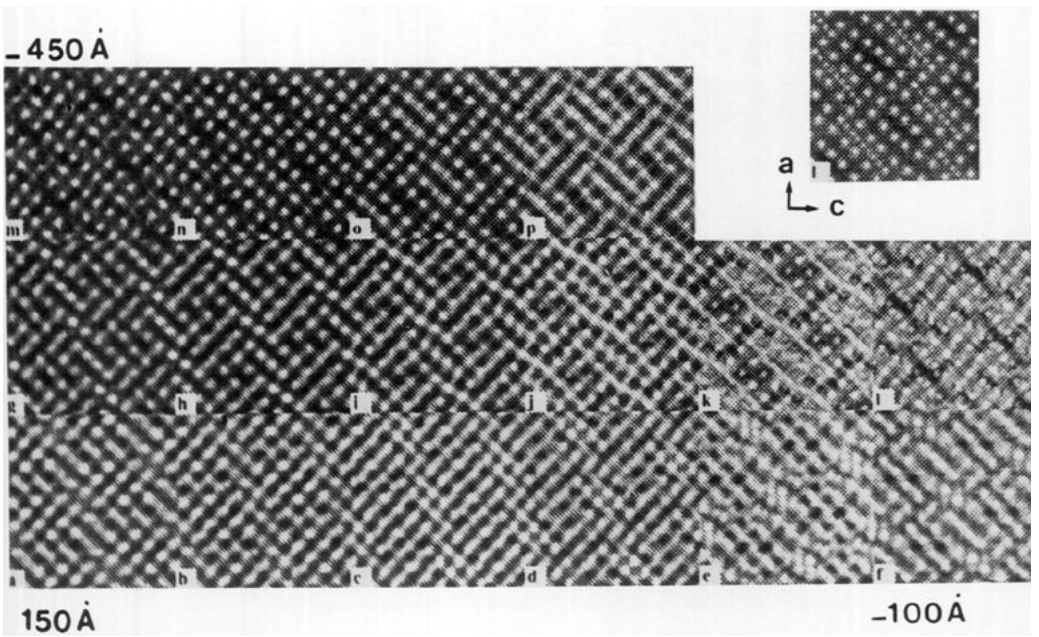

FIG. 7. Calculated through focus series for a crystal thickness $t = 33$ Å; the positional parameters are those of Table I.

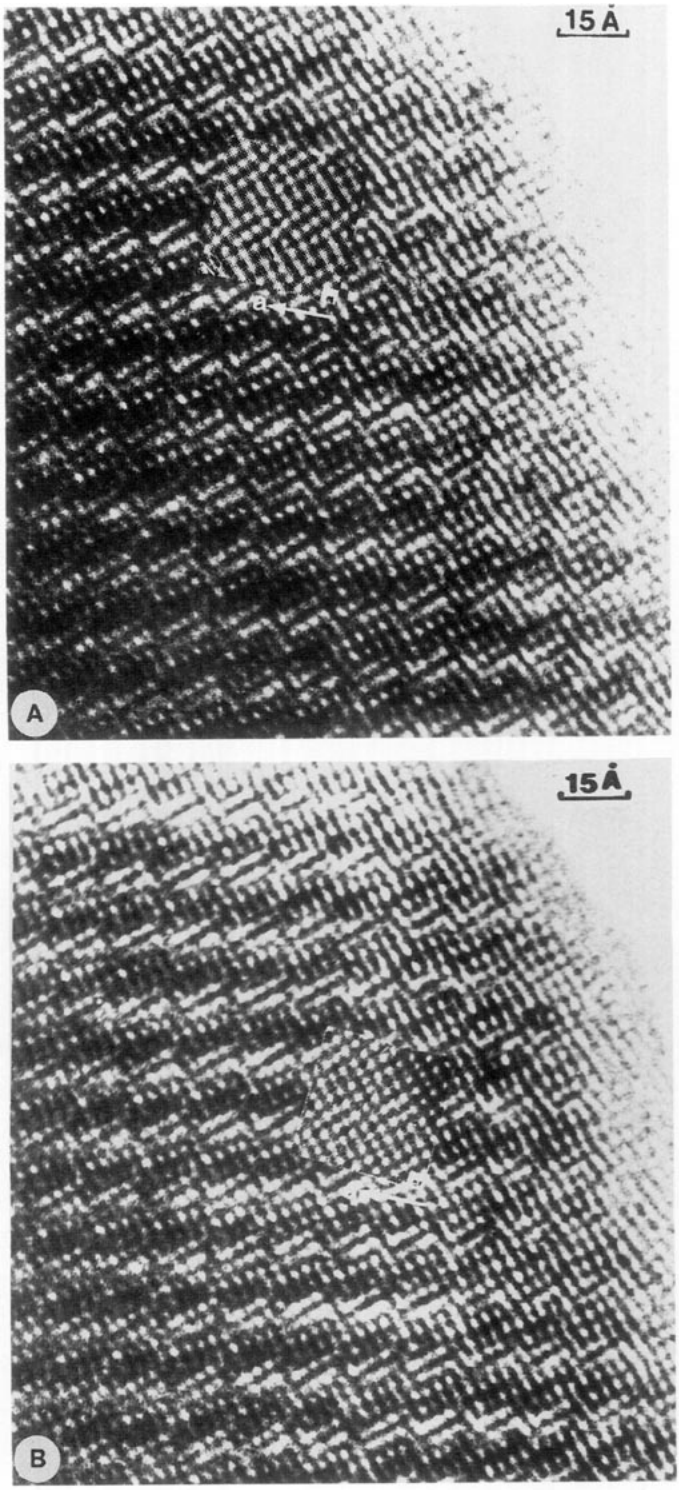

FIG. 8. Comparison between the calculated and experimental images: (a) $\Delta f \approx -250$ Å and (b) $\delta f \approx -550$ Å.

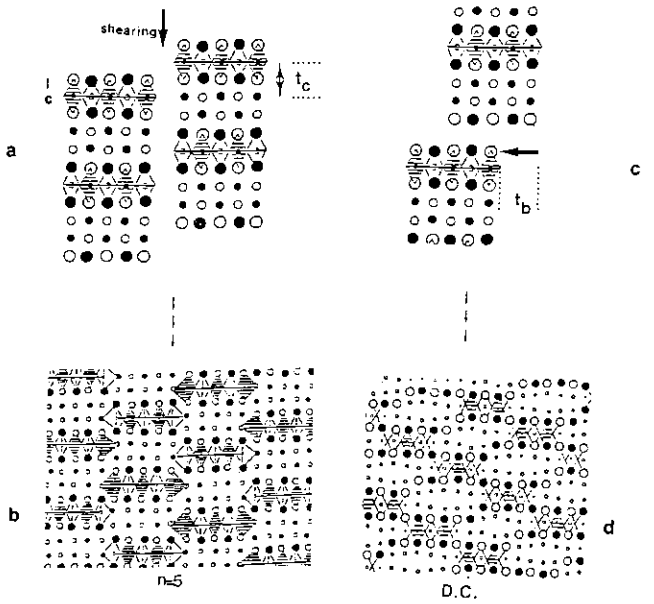

FIG. 9. Structural mechanism leading to the double collapsed phase: (a) shearing of the ideal 2201 structure along the **c** direction, (b) formation of a theoretical $n = 5$ collapsed structure, (c) translation of two layers parallel to $\mathbf{b}_{2201}$, and (d) ideal structure of the double collapsed phase.

ers (see arrows), i.e., parallel to $\mathbf{b}_{2201}$, one obtains the ideal structure of $Bi_6Ba_4Cu_2O_{15}$ (Fig. 9d). Thus this structure can be deduced from that of 2201 by a double translation, perpendicular and then parallel to the copper layers, and for this reason can be called double-collapsed phase. This second translation leads to a monoclinic cell (Fig. 9d) with an "a" parameter identical to that of the collapsed phase $n = 5$ (Fig. 9b).

In fact both structures can be described as built up from 2201-type slices which are five $(Cu_{1-x}Bi_x)O_6$ "octahedra" wide. In the $n = 5$-collapsed phase the 2201 slices are parallel to the $(010)_{2201}$ plane of the 2201-structure (Fig. 10a), whereas in the $n = 5$-double collapsed phase, $Bi_6Ba_4Cu_2O_{15}$, the 2201 slices are parallel to the $(012)_{2201}$ plane (Fig. 10b). This phenomenon is very similar to the crystallographic shearing encountered in titanium and tungsten oxides. Thus, we can distinguish the two families, collapsed and double collapsed, by the nature of the crystallographic plane where the translation appears, i.e., $\{010\}_{2201}$ or $\{012\}_{2201}$, respectively. Note that this "collapsing" operations, like the shearing operations, involve a decrease of the oxygen content with respect to the total cationic content. Another important issue deals with the junction between the different slices which are not yet clear; more specifically, the coordination of the atoms at both ends

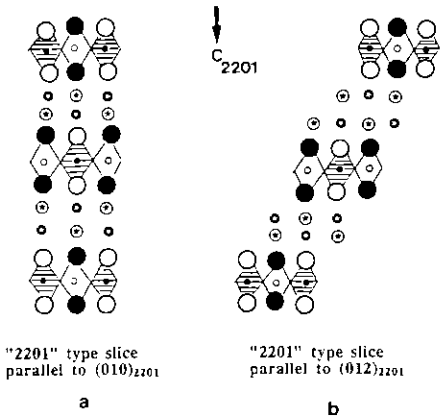

FIG. 10. Projection of 2201-type slices: (a) parallel to $(010)_{2201}$ and (b) parallel to $(012)_{2201}$.

of the octahedral copper layer is not really known in agreement with the fact that those sites one partly occupied by bismuth in any case these sites, if they are octahedral, are probably strongly distorted.

The resistivity measurements made by the classical four probe method, show that is compound is highly resistant with a resistivity close to $\rho \sim 10^8\ \Omega$ cm at room temperature.

This result is compatible with the proposed model where the CuO_2 planes are interrupt every five octahedra and with the fact that copper can be partially replaced by bismuth.

Concluding Remarks

The synthesis and HREM study, of the cuprate $Bi_6Ba_4Cu_2O_{15}$, with an original structure derived from the 2201-modulated structure by a "double collapsing" operation, opens the door to the research of oxides in this new "double collapsed" family. In fact, considering the "crystallographic collapsing planes" CCPs, with respect to the 2201-structure, we can distinguish two families of collapsed structures, the $\{010\}_{2201}$ and $\{012\}_{2201}$ families. The cuprates $Bi_{17}Sr_{16}Cu_7O_{49-\delta}$ and $Bi_{15}(Sr, Ba)_{14}Cu_6O_{42}$ represent the members $n = 8$ and 7 of the first family, whereas $Bi_6Ba_4Cu_2O_{15}$ corresponds to the member $n = 5$ of the second family. Many other members of these two families, and even of new families, corresponding to new orientations of the CCPs will certainly be isolated in the future.

References

1. H. Leligny, S. Durcok, P. Labbé, M. Ledesert, and B. Raveau, *Acta Crystallogr. Sect. B* **48,** 407 (1992).
2. G. Van Tendeloo, H. W. Zandbergen, J. Van Landuyt, and S. Amelinckx, *Appl. Phys. A* **46,** 233 (1988).
3. E. Kakayama, E. Muromuchi, Y. Uchida, A. Ono, F. Izumi, and M. Onoda, *Jpn. J. Appl. Phys.* **27,** L365 (1988).
4. P. L. Gai and P. Day, *Physica C* **152,** 335 (1988).
5. B. Raveau, C. Michel, M. Hervieu, and J. Provost, *Physica C* **153,** 1553 (1988).
6. C. Torardi, M. A. Subramanian, J. C. Calabrese, J. Gopalakrishnan, E. M. McCarron, K. J. Morrissey, T. R. Ashew, R. B. Flippen, U. Chowdry, and A. W. Sleight, *Phys. Rev. B* **38,** 225 (1988).
7. H. Von Schnering, L. Walz, M. Schwarz, W. Becker, M. Hartweg, T. Popp, B. Hettich, P. Müller, and G. Kämpf, *Angew, Chem Int. Ed. Engl.* **27,** 574 (1988).
8. K. Imai, I. Nakai, T. Kawashima, S. Sueno, and A. Ono, *Jpn. J. Appl. Phys.* **27,** 1661 (1988).
9. A. Fuertes, C. Miratvilles, J. Gonzalez-Calbet, M. Vallet-Regi, and J. Rodriguez Carjaval, *Physica C* **157,** 529 (1989).
10. M. T. Caldes, J. M. Navarro, F. Perez, M. Carrera, J. Foncuberta, M. Casan Pastor, C. Miratvilles, X. Obradors, J. Rodriguez Carjaval, J. M. Gonzalez-Calbet, M. Vallet-Regi, A. Garcia, and A. Fuertes, *Chem. Mater.* **3,** 844 (1991).
11. M. T. Caldes, M. Hervieu, A. Fuertes, and B. Raveau, *J. Solid State Chem.* **97,** 48 (1992).
12. M. T. Caldes, M. Hervieu, A. Fuertes, and B. Raveau, *J. Solid State Chem.* **98,** 301 (1992).
13. M. T. Caldes, M. Hervieu, A. Fuertes, and B. Raveau, *J. Solid State Chem.* **98,** 48 (1992).
14. Z. Hiroi, Y. Ikeda, M. Takano, and Y. Bando, *J. Mater. Res.* **6,** 435 (1991).
15. Y. Matsui, S. Takekawa, K. Kishio, A. Umezono, S. Nakamura, C. Tsuruta, and K. Ibe, *Mater. Trans. JIM* **31,** 595 (1990).
16. D. E. Cox and A. W. Sleight, *Solid State Commun.* **19,** 969, (1976).
17. A. Q. Pham, M. Hervieu, C. Michel, and B. Raveau, *J. Solid State Chem.* **98,** 426, (1992).
18. A. Q. Pham, M. Hervieu, C. Michel, and B. Raveau, *Physica C* **199,** 321 (1992)
19. A. Q. Pham, C. Michel, M. Hervieu, A. Maignan, and B. Raveau, *J. Phys. Chem. Solids,* **54,** 65 (1993).
20. M. Hervieu, C. Michel, A. Q. Pham, and B. Raveau, *J. Solid State Chem.* **104,** 289 (1993).
21. D. B. Wiles and R. A. Young, *J. Appl. Crystallogr.* **14,** 149, (1981).
22. P. A. Stadelmann, *Ultramicroscopy* **21,** 131 (1987).
23. M. W. Zandbergen, W. A. Groen, F. C. Mülhoff, G. Van Tendeloo, and S. Amelinckx, *Physica C* **156,** 325 (1988).
24. B. Domenges, M. T. Caldes, M. Hervieu, A. Fuertes, and B. Raveau, *Microscopy, Microanalysis, Microstructure* **3,** 415 (1993).